THE JOURNAL OF BIOLOGICAL CHEMISTRY
Vol. 277, No. 38, Issue of September 20, pp. 35333–35340, 2002

Printed in U.S.A.

A Novel PAAD-containing Protein That Modulates NF-κB Induction by Cytokines Tumor Necrosis Factor-α and Interleukin-1β*

Received for publication, January 15, 2002, and in revised form, June 5, 2002
Published, JBC Papers in Press, July 1, 2002, DOI 10.1074/jbc.M200446200

Loredana Fiorentino‡, Christian Stehlik‡, Vasco Oliveira, Maria Eugenia Ariza, Adam Godzik, and John C. Reed§

From The Burnham Institute, La Jolla, California 92037

PAAD domains are found in diverse proteins of unknown function and are structurally related to a superfamily of protein interaction modules that includes death domains, death effector domains, and Caspase activation and recruitment domains. Using bioinformatics strategies, cDNAs were identified that encode a novel protein of 110 kDa containing a PAAD domain followed by a putative nucleotide-binding (NACHT) domain and several leucine-rich repeat domains. This protein thus resembles Cryopyrin, a protein implicated in hereditary hyperinflammation syndromes, and was termed PAN2 for PAAD and NACHT-containing protein 2. When expressed in HEK293 cells, PAN2 suppressed NF-κB induction by the cytokines tumor necrosis factor-α (TNFα) and interleukin-1β (IL-1β), suggesting that this protein operates at a point of convergence in these two cytokine signaling pathways. This PAN2-mediated suppression of NF-κB was evident both in reporter gene assays that measured NF-κB transcriptional activity and electromobility shift assays that measured NF-κB DNA binding activity. PAN2 also suppressed NF-κB induction resulting from overexpression of several adapter proteins and protein kinases involved in the TNF or IL-1 receptor signal transduction, including TRAF2, TRAF6, RIP, IRAK2, and NF-κB-inducing kinase as well as the IκB kinases IKKα and IKKβ. PAN2 also inhibited the cytokine-mediated activation of IKKα and IKKβ as measured by *in vitro* kinase assays. Furthermore, PAN2 association with IKKα was demonstrated by co-immunoprecipitation assays, suggesting a direct effect on the IKK complex. These observations suggest a role for PAN2 in modulating NF-κB activity in cells, thus providing the insights into the potential functions of PAAD family proteins and their roles in controlling inflammatory responses.

The PAAD[1] domain is found in diverse proteins implicated in apoptosis, inflammation, and cancer (1). This protein fold, which is also known as PYRIN or DAPIN (2–4), is predicted to form an α-helical bundle resembling death domains, death effector domains, and Caspase activation and recruitment domains (CARDs). The PAAD domain thus constitutes the fourth branch of this superfamily of structurally similar protein modules, which participate in homotypic protein-protein interactions involved in signal transduction by tumor necrosis factor (TNF) family cytokine receptors and pathways connected to activation of Caspase family cell death proteases and to kinases important for induction of NF-κB family transcription factors (for reviewed, see Ref. 5).

The founding member of this family of proteins is Pyrin, which contains a PAAD domain at its N terminus followed by a B-box zinc finger and SPRY domain, a motif found in ryanodine receptors that is involved in Ca^{2+} release (6). Pyrin was identified by genetic analysis of families affected with familial Mediterranean fever, a hereditary hyperinflammatory response syndrome (7). The mutations identified in familial Mediterranean fever patients fall within the region C-terminal to the PAAD domain. Recently hereditary mutations have been identified in the *CIAS* gene, which encodes the PAAD-containing protein Cryopyrin (8). These mutations are predicted to produce mutant Cryopyrin proteins in patients affected with familial cold autoinflammatory syndrome and Muckle-Wells syndrome with mutations residing downstream of the N-terminal PAAD domain. Thus, PAAD-containing proteins appear to regulate pathways relevant to inflammation, although the molecular mechanisms are unknown. Providing further evidence of a potential link to inflammatory cell function, PAADs are also found in a group of interferon-inducible genes that includes myeloid nuclear differentiation antigen, absent in melanoma 2, and interferon-γ-inducible protein 16.

PAAD-containing proteins have also been implicated in apoptosis regulation. The PAAD domain, for example, is present in (*a*) ASC, a proapoptotic adapter protein that contains both a PAAD and a CARD and that interacts with Pyrin (9), and (*b*) NAC (CARD7/DEFCAP/NALP), an apoptosis-promoting protein that contains PAAD and CARD modules (together with additional domains) and that reportedly enhances activation of Caspase-9 either directly or indirectly through interactions with the Caspase-9 activator Apaf1 (4, 10, 11). A zebrafish Caspase also contains a PAAD within its N-terminal prodomain (12), suggesting possible links of PAADs to apoptosis. However, no evidence of direct involvement of PAAD domains in apoptosis has been obtained to date.

In total, at least 34 genes encoding PAAD-containing pro-

* This work was supported by the American-Italian Cancer Foundation, the Austrian Science Foundation (Grant J1809-Gen/J1990-Gen), the National Science Foundation (Grant DBI-0078731), the Department of Defense Breast Cancer Research Program (Grants DAMD17-00-1-0169 and BC001191), and the Gulbenkian Foundation PGDBM (Program PRAXIS XXI A.T.T.). The costs of publication of this article were defrayed in part by the payment of page charges. This article must therefore be hereby marked "*advertisement*" in accordance with 18 U.S.C. Section 1734 solely to indicate this fact.

The nucleotide sequence(s) reported in this paper has been submitted to the GenBank™/EBI Data Bank with accession number(s) AY072792.

‡ Both authors contributed equally to this work.

§ To whom correspondence should be addressed: The Burnham Institute, 10901 N. Torrey Pines Rd., La Jolla, CA 92037. Tel.: 858-646-3132; Fax: 858-646-3194; jreed@burnham.org.

[1] The abbreviations used are: PAAD, Pyrin/absent in melanoma/ASC/death domain-like; NACHT, NAIP, CIIA, HET-E, TP-1; CARD, caspase activation and recruitment domain; TNF, tumor necrosis factor; IL, interleukin; EMSA, electromobility shift assay; IKK, IκB kinase; LRR, leucine-rich repeat; EST, expressed sequence tag; HTGS, High Throughput Genome Sequences; aa, amino acid(s); HA, hemagglutinin; GST, glutathione *S*-transferase; Nik, NF-κB-inducing kinase.

teins are predicted to reside in the human genome (1).[2] Fourteen of these PAAD family proteins, including Cryopyrin, have a conserved architecture that includes an N-terminal PAAD followed by a nucleotide-binding fold known as the NACHT domain (13) and then variable numbers of leucine-rich repeat (LRR) domains as well as other domains in some members. We have termed these proteins PANs for PAAD and NACHT domain proteins. The topological organization of domains in the PANs is reminiscent of proteins previously implicated in NF-κB induction or Caspase activation such as Nod1 (CARD4), Nod2 (inflammatory bowel disease protein 1), and CLAN (Ipaf1, CARD12), which contain a CARD followed by NACHT and LRR domains (14–16). In those proteins, the N-terminal CARD is essential for the effector functions of these proteins as inducers of NF-κB or activators of Caspases. In this report, we explored the effects of one of the members of this family, PAN2, finding evidence that this protein modulates NF-κB induction via its PAAD domain.

MATERIALS AND METHODS

Bioinformatics—Using the sequence of the 100-residue N-terminal region of the Pyrin protein, a cascade of PSI-BLAST searches was performed using new hits as queries for subsequent searches until no new hits were found. This procedure, called Saturated BLAST (17), revealed several genomic loci and EST clones potentially capable of encoding PAAD domains in the publicly available nucleotide databases (HTGS, Genome Survey Sequences, EST, and draft human genome). For genomic data, the amino acid sequences of the predicted PAAD-containing proteins were tentatively deduced using the GENSCAN program for intron-exon prediction (18). Several examples were found of proteins that are predicted to contain a PAAD domain together with a NACHT domain, thus constituting members of the PAN family. In this report, we describe PAN2, which is encoded within the genomic locus AC022066 on chromosome 19 with partial or complete open reading frames for this protein encompassed in representative EST clones BE018433, AA421452, and AI204456.

Plasmids—Plasmids were generated using PCR procedures with primers designed to incorporate appropriate restriction enzyme sites. Polymerase chain reaction products were then digested and cloned into pcDNA3Myc vector. All plasmids were sequence-verified.

Reverse Transcriptase-PCR Assays—Panels of first-strand cDNAs (CLONTECH Panel I and II) generated from the mRNA of various human tissues were used as templates to amplify a region of PAN2 corresponding to the nucleotide-binding domain (amino acids (aa) 147–465) using the forward and reverse oligonucleotides 5′-CCACGTACAGTGATTATTCAAGGACC-3′ and 5′-CAAATAGAACAAGGCGGCACAGA-3′, respectively. Alternatively, total RNA from HeLa cells was subjected to reverse transcriptase-PCRs to amplify a partial clone of PAN2 (aa 1–620) using the following oligonucleotides: forward, 5′-ATGGCAGCCTCTTTCTTCTCTGATTTT-3′; reverse, 5′-CGACGTAGAGCTGTGTTCATCCTCTTTCTTAA-3′. The resulting PCR product was excised from agarose gels and cloned into pcDNA3Myc, and its identity was confirmed by DNA sequencing.

Antibody Generation and Immunoblot Analysis—A polyclonal anti-PAN2 antiserum was generated by repeated immunization of rabbits with an 18-mer synthetic peptide spanning aa 139–157 of PAN2 protein (FAPKETGKQPRTVIIQGPQ) conjugated to maleimide-activated carrier proteins keyhole limpet hemocyanin and ovalbumin (Pierce). Total protein lysates from various untransfected cell lines, from 293 cells transiently transfected with Myc-PAN2 (as a positive control), and from stably transfected 293-Neo and 293-PAN2 cell lines were prepared, normalized for total protein content (100 μg), and size-fractionated in an 8% polyacrylamide gel under standard SDS-PAGE conditions. Proteins were then transferred onto nitrocellulose membranes (Bio-Rad) and incubated with a 1:1000 (v/v) dilution of anti-PAN2 antiserum or anti-β-actin antibody (Sigma). Detection was accomplished by enhanced chemiluminescence.

Luciferase Reporter Gene Assays—Typically 1×10^4 HEK293 cells were plated in 96-well plates and transfected using Superfect transfection reagent (Qiagen) following the manufacturer's recommended protocol. For NF-κB reporter assays, cells were transfected with 50 ng of pNF-κB-luc and 10 ng of pTK-RL reporter vectors (Stratagene) and various amounts of the relevant expression plasmids as described in the figure legends, maintaining the total amount of DNA constant using pcDNA3Myc empty vector. The β-catenin reporter assays were performed in the same way using 100 ng of β-catenin reporter plasmid, 10 ng of pTK-RL, and 500 ng of β-catenin expression vector (19). At 36 h after transfection, cells were treated with TNFα or IL-1β (both 20 ng/ml) for 6 h where indicated. Activities from firefly and *Renilla* luciferases were assayed using the Dual-Luciferase Reporter Assay System (Promega).

Stable Transfections—For stable transfections, 5×10^5 HEK293 cells were seeded in 6-cm plates and transfected with 2.5 μg of pMyc-PAN2 or pMyc empty vector using LipofectAMINE Plus (Invitrogen). After 2 days, transfected cells were split 1:3 into 10-cm dishes and grown in the presence of 1 mg/ml G418 until individual colonies appeared. Several well separated clones were recovered and analyzed by immunoblotting to assess relative levels of PAN2. One clone expressing PAN2 was identified (293-PAN2) and used to perform electromobility shift assays (EMSAs). A clone transfected with pcDNA3Myc plasmid (293-Neo) was also randomly picked for use as a control.

Co-immunoprecipitation Assays—293T cells were seeded at a density of 2×10^6 cells/10-cm plate the day before transfection. Cells were transfected with 6 μg of various combinations of plasmids as described above and then harvested 36 h after transfection. Alternatively stably transfected 293-Neo and 293-PAN2 cells were used. Cells were lysed in 400 μl of immunoprecipitation lysis buffer (50 mM Tris (pH 8.0), 150 mM NaCl, 1% Nonidet P-40, 1 mM dithiothreitol) containing protease inhibitors (Roche Molecular Biochemicals). After centrifugation, clarified lysates were subjected to immunoprecipitation with anti-HA or anti-Myc antibodies immobilized on agarose (Santa Cruz Biotechnology) for 3 h at 4 °C followed by three washes in immunoprecipitation lysis buffer. Immune complexes were subjected to SDS-PAGE, transferred to nitrocellulose membranes (Bio-Rad), and analyzed by immunoblotting using anti-Myc or anti-IκB kinase α (IKKα) antibodies (Santa Cruz Biotechnology).

EMSAs—Stably transfected 293-Neo and 293-PAN2 cells were seeded in 10-cm plates, cultured overnight in 1% fetal bovine serum, and then left untreated or treated with 20 ng/ml TNFα for 30 min or with 100 ng/ml IL-1β for 2 h. Nuclear extracts were prepared from these cells, and EMSAs were carried out as described previously (20). Briefly, a double-stranded oligonucleotide containing a consensus NF-κB binding site (Promega) was end-labeled with [γ-^{32}P]ATP (PerkinElmer Life Sciences) using T4 polynucleotide kinase (Amersham Biosciences). After purification with MicroSpin G-25 columns (Amersham Biosciences), the labeled probe (15 fmol) was incubated with 2 μg of nuclear extracts for 25 min at room temperature. The nuclear extracts from TNF-treated cells were also incubated with specific antibodies recognizing the NF-κB subunits p65 and p50 (Santa Cruz Biotechnology) before the binding reaction or with 100-fold molar excess of unlabeled DNA probe as specific competitor. All complexes were separated by electrophoresis in non-denaturing 5% polyacrylamide gels at 4 °C. After drying, gels were exposed to x-ray film at −70 °C.

Kinase Assays—293 cells were transfected with 0.5 μg of FLAG-IKKα expression vector and either pMyc empty vector, increasing amounts of pMyc-PAN2, or 0.5 μg of the indicated Myc-tagged PAN2 deletion mutants. At 36 h after transfection, cells were left untreated or treated with 20 ng/ml TNFα for 15 min. Cells were resuspended in kinase assay lysis buffer (50 mM Tris (pH 7.5), 200 mM NaCl, 2 mM EDTA, 1% Brij 97 (polyoxyethylene alcohol), 10% glycerol, 0.5% Triton X-100) supplemented with a mixture of protease inhibitors (Roche Molecular Biochemicals) and 2 mM phenylmethanesulfonyl fluoride-α-toluenesulfonyl fluoride, 50 μM dithiothreitol, and 1 mM Na_3VO_4. Lysates were immunoprecipitated with anti-FLAG antibody conjugated to agarose (Sigma) for 3 h at 4 °C. The immunoprecipitates were washed three times in lysis buffer and then washed once with kinase buffer (20 mM Hepes (pH 7.4), 5 mM $MgCl_2$, 2 mM $MnCl_2$, 1 mM dithiothreitol, 0.1 mM Na_3VO_4, 20 mM NaF, and 10 mM β-glycerophosphate). Kinase assays were performed in 15 μl of kinase buffer containing 5 μM ATP, 5 μCi of [γ-^{32}P]ATP and 1 μg of GST-IκBα-(1–54) for 20 min at 30 °C. Reactions were stopped by adding 3 μl of 5× Laemmli buffer and boiling for 5 min. Samples were subjected to 12% SDS-PAGE, transferred to nitrocellulose membranes, and exposed to x-ray film. The same membranes were subsequently probed with anti-FLAG antibody to determine the amounts of FLAG-IKKα present. Cell lysates were normalized for total protein content (30 μg) and analyzed by immunoblotting to confirm expression of Myc-PAN2 and Myc-tagged PAN2 mutants.

[2] A. Godzik and J. C. Reed, unpublished data.

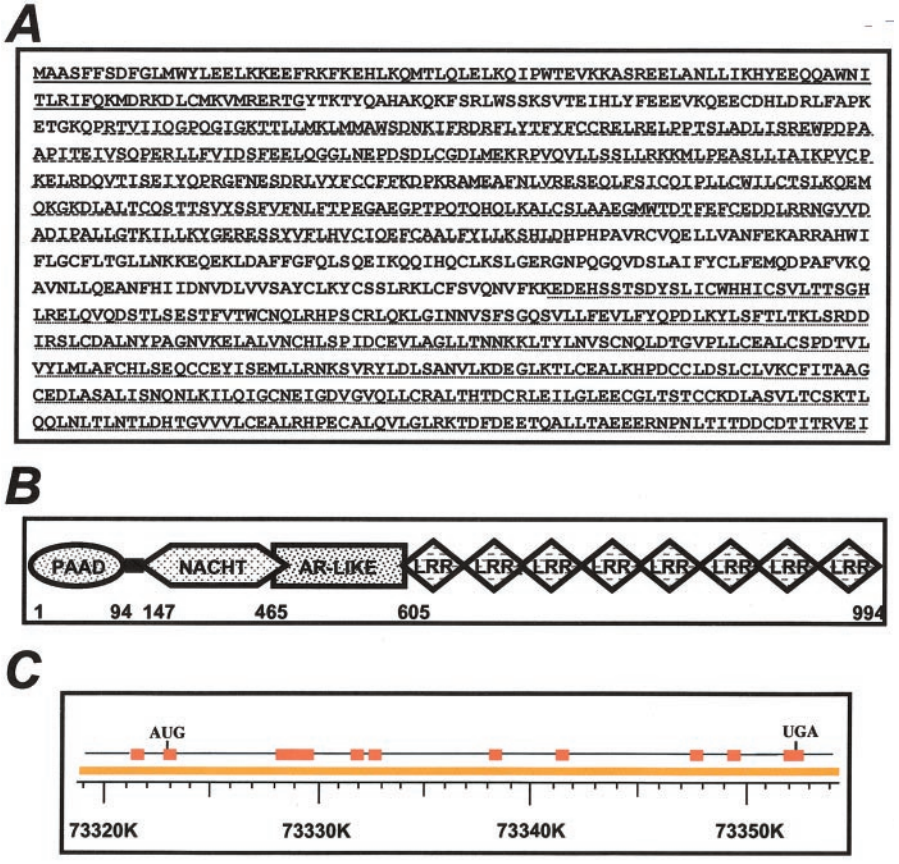

FIG. 1. **Predicted amino acid sequence and genomic structure of *PAN2* gene.** *A*, the predicted amino acid sequence of the 994-aa PAN2 protein is presented. The PAAD, NACHT, and LRRs are indicated by *underlining* using *solid*, *dashed*, and *dotted lines*, respectively. *B*, schematic diagram of the structural features of PAN2. The PAAD domain comprises aa 1–94, the NACHT domain aa 147–465, and the LRR domain aa 605–995. Between the NACHT and LRRs is a domain that is commonly associated with NACHT-containing proteins and shares sequence similarity with a putative angiotensin receptor (*AR*) (L. Jaroszewski and A. Godzik, unpublished). *C*, the exon-intron organization of the *PAN2* gene is presented as deduced from cDNA sequencing and comparison to the Human Genome Database genomic sequence.

RESULTS

Molecular Cloning of Human PAN2, a Novel PAAD- and NACHT-containing Protein—Using bioinformatics strategies, we identified several genes potentially capable of encoding predicted proteins having PAAD and NACHT domains, thus constituting members of the PAN family, which includes NAC, Cryopyrin, PAN2, and 11 other related proteins, all sharing significant sequence homology. An HTGS clone (accession number AC022066) allowed us to obtain genomic sequence data for *PAN2*, and the analysis of this HTGS clone with the GENSCAN program provided an intron-exon prediction encompassing the N-terminal segment of *PAN2*. To independently verify expression of *PAN2*, a set of primers was designed based on the predicted partial cDNA sequence and used to perform reverse transcriptase-PCR using HeLa cell RNA. The PCR product was cloned into a plasmid (pcDNA3Myc) and sequenced, verifying that it contained nucleotides 1–1860 of the *PAN2* cDNA.

To further define the expressed product of the *PAN2* gene, a BLAST search of the human EST database was performed using this partial cDNA as a query. Several EST clones were identified that overlapped all or part of the *PAN2* partial cDNA sequence. One of these clones contained an insert of 3.4 kbp and was obtained for complete sequencing, revealing an open reading frame of 2985 nucleotides encoding the 994-aa PAN2 protein (Fig. 1*A*). The authenticity of this open reading frame was confirmed by *in vitro* translation (not shown). The initiating AUG codon of this open reading frame was preceded by a 5′-untranslated region of 57 bp, whereas the stop codon (2985 bp) was followed by a 3′-untranslated region of 348 bp and a poly(A) tail (submitted to GenBank™, accession number AY072792). This cDNA is substantially similar to a recently deposited sequence (GenBank™ accession number AF442488). The predicted PAN2 protein contains a PAAD domain at its N terminus (aa 1–94), a central NACHT domain (aa 147–465), and eight tandem C-terminal LRR domains (aa 605–995) (Fig. 1*B*).

Using the cDNA sequence of the 3.4-kbp *PAN2* clone, we deduced the exon-intron organization of the gene (Fig. 1*C*). The *PAN2* gene spans 30 kbp on chromosome 19 and contains at least 10 exons, including 9 coding and at least 1 non-coding exon (the possibility of additional 5′-untranslated region exons cannot be excluded). Interestingly, none of the standard gene prediction programs was able to predict the complete *PAN2* cDNA sequence from genomic data. Most often the PAAD-containing exon is predicted to be part of an intron or a promoter region in an upstream gene coding for an uncharacterized protein from the Mucin family. Since the Mucin family contains multiple copies of a 50-aa repeat, it is possible that the genomic sequence in this region was not assembled correctly.

To analyze the expression of *PAN2*, first-strand cDNAs generated from equivalent amounts of RNA from a variety of normal human tissues were used as templates to amplify a region of the *PAN2* cDNA corresponding to the NACHT domain (aa 147–465). This analysis revealed that *PAN2* is expressed at highest levels in spleen but also in placenta, lung, liver, kidney, pancreas, and thymus (Fig. 2*A*).

We also generated a polyclonal antiserum raised against a peptide corresponding to aa 139–157 of PAN2. This antiserum recognized PAN2 as a single band of ~110 kDa (which is in agreement with the predicted molecular mass of 113.4 kDa). The slower migration of plasmid-derived PAN2 compared with the endogenous protein is due to the Myc epitope tag appended to the latter (Fig. 2*B*). Immunoblot analysis of a panel of human cell lines of various tissue origins revealed widespread expression of the PAN2 protein (Fig. 2*C*).

Regulation of NF-κB Activity by PAN2—We sought evidence that PAN2 might modulate activation of Caspases involved in either apoptosis or inflammation but failed to observe consist-

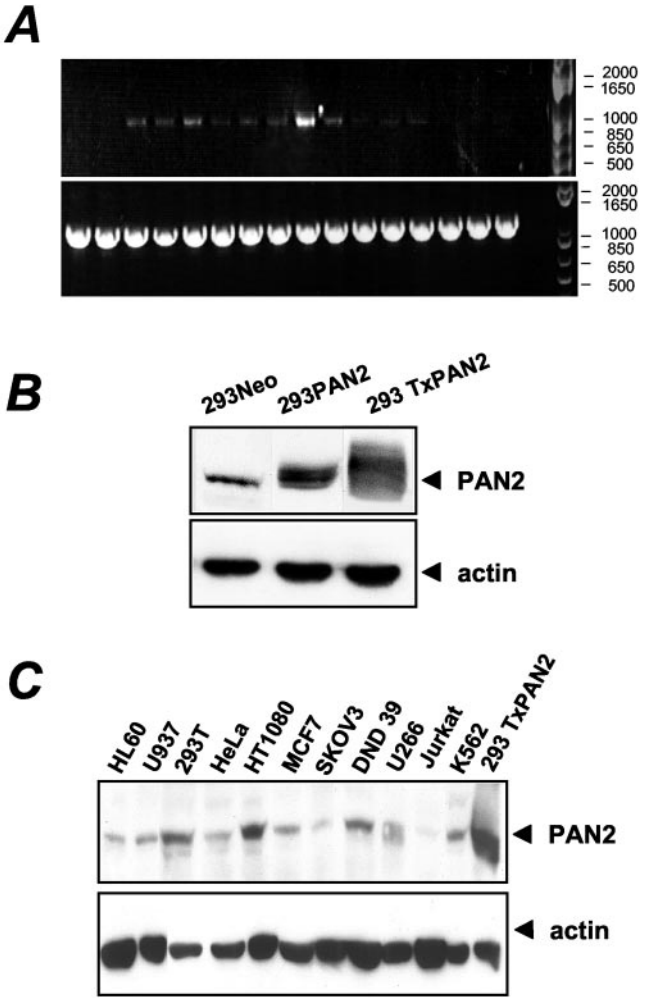

FIG. 2. **PAN2 expression in human tissues and cell lines.** *A*, first-strand cDNAs (CLONTECH) were used as templates for amplifying either a region of PAN2 corresponding to the NACHT domain (aa 147–465) (*top*) or glyceraldehyde-3-phosphate dehydrogenase as a control (*bottom*). PCR products were analyzed by agarose gel electrophoresis and visualized by UV illumination of ethidium bromide-stained gels. *Lane 1*, heart; *lane 2*, brain, *lane 3*, placenta; *lane 4*, lung; *lane 5*, liver; *lane 6*, skeletal muscle; *lane 7*, kidney; *lane 8*, pancreas; *lane 9*, spleen; *lane 10*, thymus; *lane 11*, prostate; *lane 12*, testis; *lane 13*, ovary; *lane 14*, intestine; *lane 15*, colon; *lane 16*, peripheral blood lymphocytes; *lane 17*, negative control reaction performed without cDNA. Molecular weight markers are shown at *right* in bp. *B*, total protein lysates (80 μg) were prepared from stably transfected 293-Neo and 293-PAN2 (*lanes 1* and *2*) and from 293 cells transiently transfected with Myc-PAN2 plasmid (*lane 3*) and analyzed by immunoblot for PAN2 protein expression. The same membrane was then stripped and reprobed for β-actin as a loading control. *C*, total protein lysates (100 μg) were prepared from the indicated human cell lines and from 293 cells transiently transfected with Myc-PAN2 plasmid (positive control, *rightmost lane*) and analyzed as in *B*.

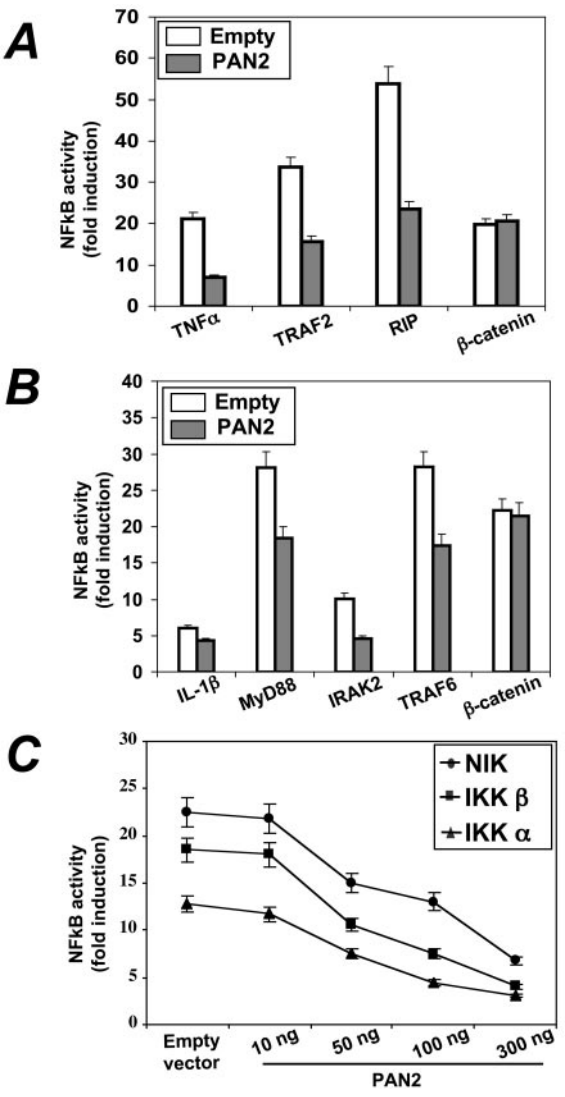

FIG. 3. **PAN2 inhibits NF-κB induction.** *A* and *B*, HEK293 cells were seeded into 96-well plates and transfected on the following day with 50 ng of pNF-κB-luc and 10 ng of pTK-RL reporter gene plasmids together with 400 ng of pcDNA3Myc empty vector (*Empty*, *white bars*) or 400 ng of pcDNA3Myc-PAN2 (*PAN2*, *gray bars*) and stimulated for 6 h with TNFα (*A*) or IL-1β (*B*). Alternatively cells were co-transfected with 100 ng of plasmids encoding TRAF2, TRAF6, MyD88, RIP, or IRAK2. The *last bars* in each panel represent a control in which 100 ng of β-catenin-luc reporter gene plasmid and 500 ng of β-catenin-encoding plasmid were transfected. After 36 h, cells were harvested, and the ratio of firefly to *Renilla* luciferase activity was determined for each sample. *Numbers* indicate -fold induction of the NF-κB reporter gene above base line (mean ± S.D., $n \geq 3$). *C*, HEK293 cells were co-transfected with 50 ng of pNF-κB-luc and 10 ng of pTK-RL reporter gene plasmids together with 80 ng of pcDNA3Myc-Nik, pcDNA3HA-IKKα, or pcDNA3HA-IKKβ and with either pcDNA3Myc empty vector or various amounts of pcDNA3Myc-PAN2 (ranging from 10 to 300 ng), holding total DNA constant at 360 ng per transfection. Luciferase assays were performed 36 h after transfection as described above (mean ± S.D., $n \geq 3$).

ent effects in transient transfection assays (not shown). Because some members of the PAAD family proteins are involved in hyperinflammatory diseases (21), we asked whether PAN2 could regulate NF-κB induction given that activation of this family of heterodimeric transcription factors is commonly involved in immune and inflammatory cell biology (for review, see Ref. 22). To explore this possibility, we transiently transfected HEK293 cells with a PAN2-encoding plasmid together with a NF-κB-dependent luciferase reporter gene plasmid. Cells were stimulated with IL-1β or TNFα, or they were co-transfected with plasmids encoding various signal transducing proteins within the TNFα receptor (TRAF2 and RIP) or the IL-1β receptor/Toll family receptor (MyD88, IRAK2, and TRAF6) pathway (for review, see Ref. 23). Under these experimental conditions, PAN2 potently inhibited NF-κB induction by TNFα (Fig. 3*A*) and to a lesser extent by IL-1β (Fig. 3*B*). PAN2 overexpression also markedly reduced NF-κB activity induced by intracellular adapter proteins (TRAF2, TRAF6, and MyD88) and kinases (RIP and IRAK2) that functionally connect TNF and IL-1R receptors to NF-κB responses (Fig. 3, *A* and *B*). These effects of PAN2 were specific in that the activity of other transcription factors such as β-catenin and p53 were not suppressed (Fig. 3 and data not shown). Moreover, immunoblotting confirmed that PAN2 did not interfere with the

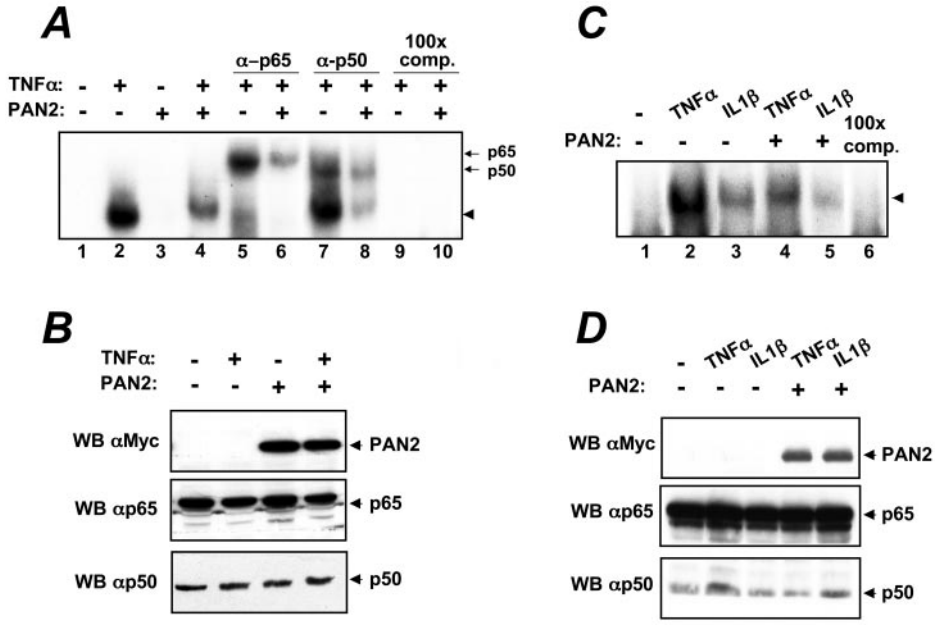

FIG. 4. **PAN2 inhibits the DNA binding activity of NF-κB.** *A*, 293-Neo (*lanes 1*, *2*, *5*, *7*, and *9*) or 293-PAN2 (*lanes 3*, *4*, *6*, *8*, and *10*) cells were cultured with (*lanes 2*, *4*, and *5–10*) or without (*lanes 1* and *3*) TNFα (20 ng/ml) for 30 min before producing nuclear extracts. EMSA was performed using 2 μg of nuclear extracts and a ^{32}P-labeled double-stranded oligonucleotide probe containing a NF-κB DNA binding site. Nuclear extracts from stimulated cells were also incubated with specific antibodies recognizing the NF-κB subunit p65 (*lanes 5* and *6*) or p50 (*lanes 7* and *8*). The *upper arrows* indicate the antibody-shifted complexes. The specificity of the band corresponding to NF-κB (*arrowhead*) was determined using a 100-fold molar excess of unlabeled DNA probe as specific competitor (*100x comp.*, *lanes 9* and *10*). *B*, total cellular extracts from *A* (*lanes 1–4*) were subjected to immunoblot analysis to confirm equal expression of PAN2, p65, and p50. *C*, as in *A*, EMSA was performed on Myc or Myc-PAN2 stably transfected 293 cells not treated (*lane 1*) or treated with TNFα (20 ng/ml) for 30 min (*lanes 2* and *4*) or IL-1β (100 ng/ml) for 2 h (*lanes 2* and *5*). The specificity of the band corresponding to NF-κB (*arrowhead*) was determined using a 100-fold molar excess of unlabeled DNA probe as specific competitor (*100x comp.*, *lane 6*). *D*, total cellular extracts from *C* were analyzed by Western blotting as described in *B*. *WB*, Western blot.

production of the TRAF2, TRAF6, MyD88, RIP, or IRAK proteins in transfected cells (not shown), excluding reduced expression as a trivial explanation for the observations.

NF-κB induction results from activation of the IKK complex, which phosphorylates the NF-κB inhibitor IκB and targets it for ubiquitination and proteasome-mediated degradation, thereby releasing NF-κB (for review, see Ref. 24). The IKK complex contains two kinases, IKKα and IKKβ. These kinases are known to become activated by Nik, a TRAF-binding protein kinase implicated in NF-κB induction by both TNF and IL-1/Toll family receptors (20). We therefore asked whether PAN2 overexpression alters the ability of Nik, IKKα, and IKKβ to induce NF-κB activity in cells. Using transient transfection and reporter gene assays, similar to the experiment described above, we showed that PAN2 caused dose-dependent suppression of NF-κB induction by these kinases (Fig. 3*C*). These observations imply that PAN2 interferes with a distal event at a point of convergence of cytokine signal transduction pathways involved in NF-κB induction.

To determine whether the observed reduction in NF-κB activity correlated with reduced NF-κB DNA binding activity in PAN2-overexpressing cells, an EMSA was performed using a ^{32}P-labeled double strand DNA oligonucleotide encompassing NF-κB binding sites. Nuclear extracts were prepared from cells that had been stably transfected with either control or PAN2-encoding plasmids and then stimulated with TNFα or IL-1β. Incubation of the nuclear extracts with ^{32}P-labeled NF-κB probe then permitted measurements of the relative levels of the NF-κB DNA binding activity. As shown in Fig. 4*A*, TNFα stimulated increases in NF-κB DNA binding activity in control transfected cells. In contrast, NF-κB DNA binding activity was markedly reduced in cells stably overexpressing PAN2. Incubating the protein-DNA complexes with antibodies recognizing various members of the Rel/NF-κB family of transcription factors provided evidence that p50 and p65 subunits of NF-κB are included in the DNA-protein complexes, producing a supershift effect in EMSAs. Similar results were obtained by stimulating the stably transfected cells with IL-1β (Fig. 4*C*). Although IL-1β is less potent than TNFα at inducing NFκB in these cells, the extent of inhibition by PAN2 was comparable for these two cytokines. Immunoblot analysis of cell lysates revealed that 293-Neo and 293-PAN2 cell lines express equivalent levels of NF-κB p50/p65 proteins, excluding the possibility that a reduced level of these proteins accounts for the results (Fig. 4, *B–D*). We conclude from these experiments that PAN2 inhibits the induction of NF-κB DNA binding activity by TNFα and IL-1β.

The PAAD Domain of PAN2 Is Sufficient for Suppression of NF-κB Activity—To explore the region within PAN2 responsible for inhibition of NF-κB activation, we constructed plasmids encoding Myc-tagged deletion mutants of PAN2 containing the PAAD domain alone (aa 1–94), a mutant lacking the PAAD domain (ΔPAAD, aa 147–994), a mutant lacking the leucine-rich repeats (ΔLRR, aa 1–620), and a mutant containing only the LRRs (aa 605–994) (Fig. 5*A*). These plasmids were then transiently expressed in HEK293 cells in equal amounts using a plasmid dose at which PAN2 suppresses TNFα induction of NF-κB by ~50% so that either loss or gain of function could be detected. As shown in Fig. 5*B*, TNFα-mediated NF-κB activation was inhibited to similar extents by full-length PAN2, the PAAD domain only, and PAN2 lacking the LRRs. In contrast, the PAN2 mutant lacking the PAAD domain displayed reduced activity, and a mutant encompassing only the LRR was completely inactive at suppressing TNFα-mediated induction of NF-κB activity. The failure of the LRR region to inhibit TNFα-mediated NF-κB induction was not due to a failure to produce comparable amounts of this protein compared with the other PAN2 mutants as demonstrated by immunoblot analysis (Fig. 5*C*).

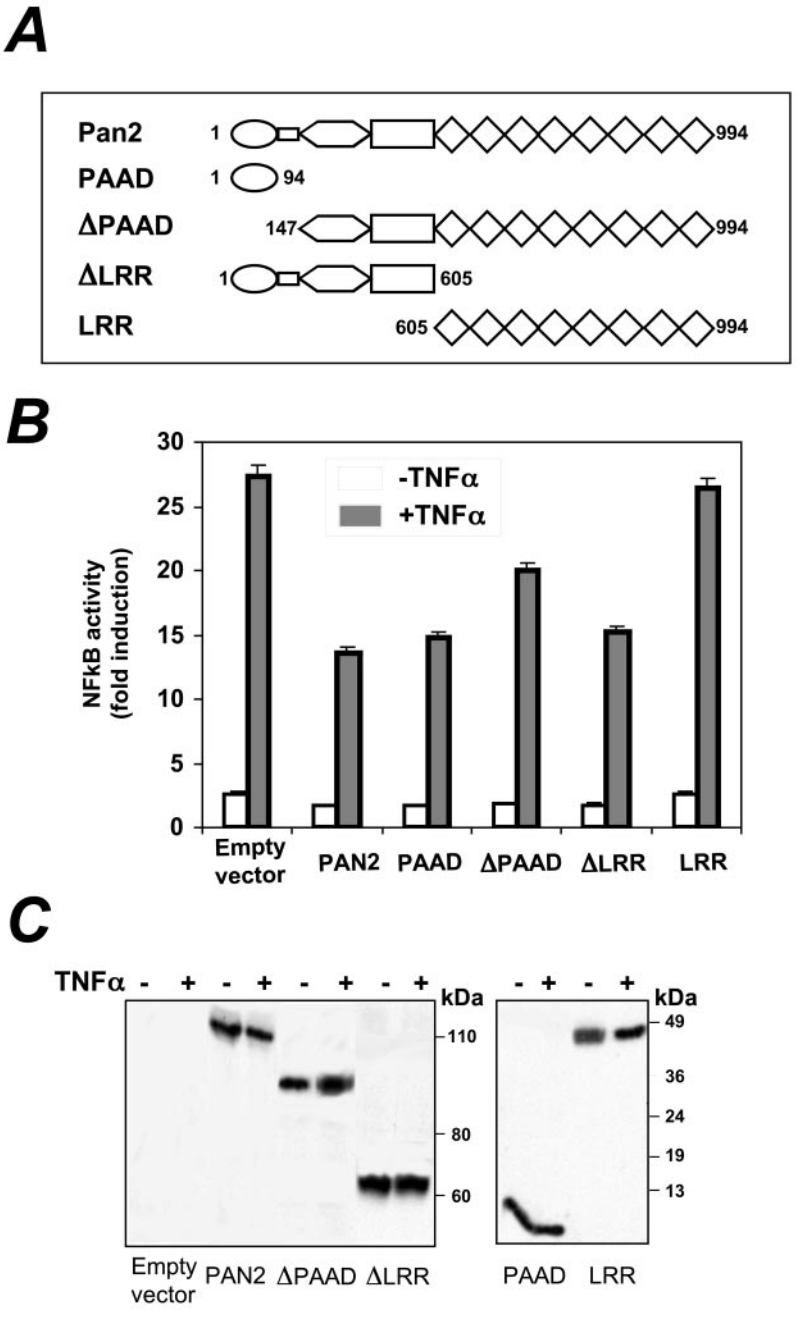

FIG. 5. **Structure-function analysis of PAN2.** *A*, a schematic representation of Myc-tagged PAN2 deletion mutants is depicted. *B*, HEK293 cells were transfected with 50 ng of pNF-κB-luc, 10 ng of pTK-RL reporter vectors, and either 400 ng of pcDNA3Myc empty vector or the same amount of the indicated Myc-tagged PAN2 deletion mutants. At 36 h after transfection, cells were either left untreated (*white bars*) or stimulated for 6 h with TNFα (*gray bars*). Cells were then harvested, and luciferase activities were determined as described under "Materials and Methods." Data indicate the -fold induction of luciferase activity (mean ± S.D., $n = 3$). *C*, immunoblot analysis of PAN2 mutants was performed. Lysates from transfected HEK293 cells were normalized for total protein content (30 μg) and subjected to SDS-PAGE/immunoblot analysis using anti-Myc antibody with enhanced chemiluminescence-based detection. Molecular mass markers are indicated at *right*.

PAN2 Associates with and Inhibits Activation of IKKs—Since the functional analysis of PAN2 suggested that it can suppress NF-κB activity induced by overexpression of IKKα or IKKβ, we explored whether PAN2 might associate with components of the IKK complex. Using lysates from HEK293 cells in which PAN2 was co-expressed with epitope-tagged IKKα, IKKβ, or IKKγ, co-immunoprecipitation assays were performed, revealing association of IKKα with PAN2 (Fig. 6*A*). Under these conditions, association of PAN2 with IKKβ or IKKγ was not detected. Immunoblot analysis of the lysates confirmed production of IKKα, IKKβ, and IKKγ at comparable levels, excluding differences in the levels of expression of these proteins as an explanation for the selective association with IKKα. We were also able to detect the interaction of PAN2 with the endogenous IKKα (Fig. 6*B*). In contrast to IKKα, PAN2 did not co-immunoprecipitate with other proteins such as p105 or Nik (not shown), further demonstrating specificity.

Next we measured the effect of PAN2 on the activity of IKKα using *in vitro* kinase assays. For these experiments, HEK293 cells were transiently transfected with plasmids encoding epitope-tagged IKKα or IKKβ together with either a control plasmid or various amounts of a PAN2-encoding plasmid. After 36 h, cells were left untreated or stimulated with TNFα for 15 min, then cell lysates were prepared, and either IKKα or IKKβ was immunoprecipitated. The resulting immunoprecipitates were then used for *in vitro* kinase assays where they were incubated with the exogenous substrate (GST-IκBα-(1–54)) in the presence of [γ-^{32}P]ATP. The kinase reaction products were then analyzed by SDS-PAGE, examining phosphorylation of GST-IκBα substrate as well as phosphorylation of the kinases. Furthermore, the immunoprecipitates were subjected to SDS-PAGE/immunoblot analysis to verify loading of equivalent amounts of proteins.

As shown in Fig. 7*A*, TNFα induced increases in both the phosphorylation and kinase activity of IKKα in control-transfected cells. In contrast, TNFα-inducible IKKα activity and

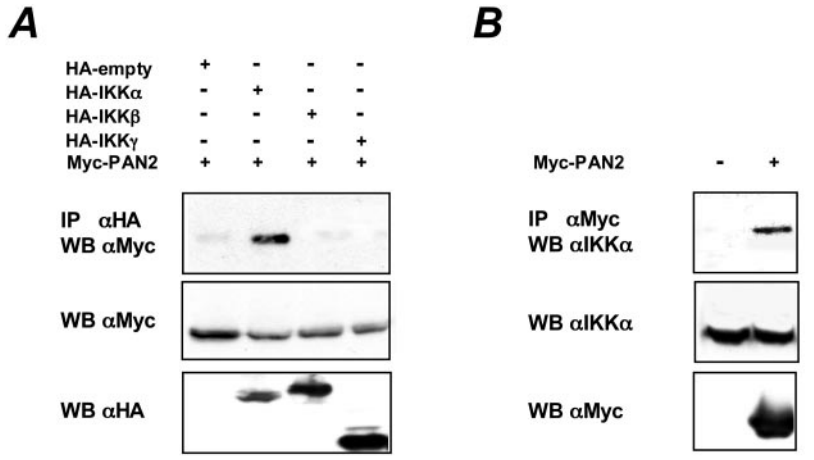

FIG. 6. **PAN2 interacts with IKKα.** *A*, 293T cells were transfected with 4 μg of pcDNA3Myc-PAN2 together with 4 μg of HA empty vector (*lane 1*) or 4 μg of plasmids encoding HA-IKKα, HA-IKKβ, or HA-IKKγ (*lanes 2–4*). After 36 h, cell lysates were prepared and subjected to immunoprecipitation (*IP*) with anti-HA antibody. The resulting immune complexes were then analyzed by SDS-PAGE/immunoblotting using anti-Myc antibody (*top*). Alternatively lysates were run directly on gels (25 μg of protein) and analyzed by immunoblotting (*WB*) using anti-Myc (*middle*) or anti-HA (*bottom*) to confirm expression of proteins. *B*, 293-Neo or 293-PAN2 stable cell lysates were immunoprecipitated (*IP*) with anti-Myc antibody. Immune complexes were then analyzed by immunoblotting using anti-IKKα antibody (Santa Cruz Biotechnology) to detect the association of PAN2 with the endogenous IKKα (*top*). Alternatively lysates were run directly on gels (25 μg of protein) and analyzed by immunoblotting (*WB*) using anti-IKKα (*middle*) or anti-Myc (*bottom*) to confirm expression of proteins. *WB*, Western blot.

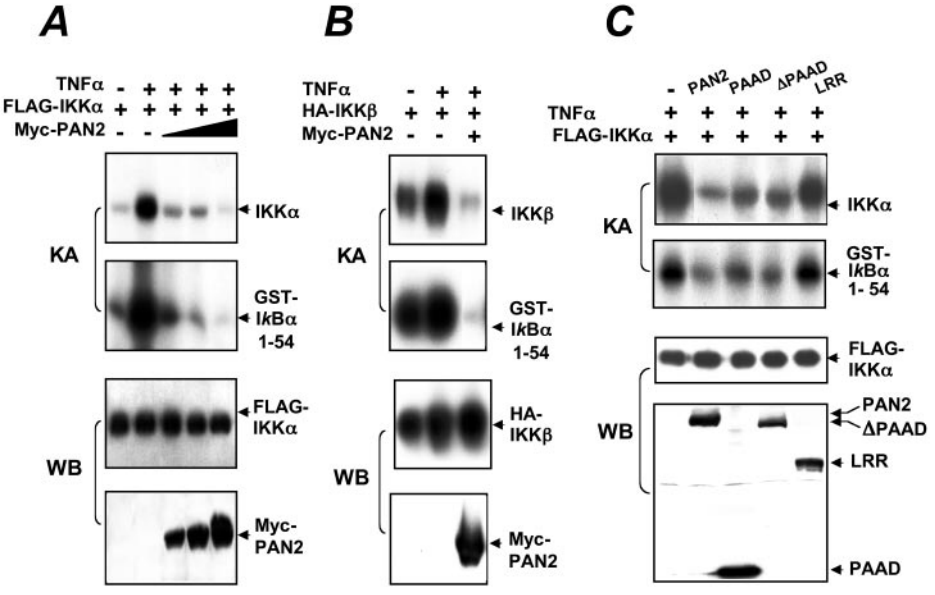

FIG. 7. **PAN2 inhibits IKKs activity.** *A*, HEK293 cells were co-transfected with 0.5 μg of FLAG-IKKα and either pcDNA3Myc empty vector (*lanes 1* and *2*) or increasing amounts (0.5, 1, and 2.5 μg) of Myc-PAN2 (*lanes 3–5*). After 36 h, cells were cultured with (+) or without (−) 20 ng/ml TNFα for 15 min, and cell lysates were prepared for immunoprecipitation with anti-FLAG antibody. Immune complexes were used for *in vitro* kinase assays (*KA*) measuring IKKα phosphorylation (*top*) and phosphorylation of exogenous substrate GST-IκBα-(1–54) (*second from top*). Immunoblot analysis of the immune complexes with anti-FLAG antibody (*third from top*) and of lysates with anti-Myc antibody (*bottom*) was performed to contrast the amounts of FLAG-IKKα immunoprecipitated and the relative amounts of Myc-PAN2 produced, respectively. *B*, similar experiments were performed for IKKβ using 0.5 μg of HA-IKKβ- and 2.5 μg of Myc-PAN2-encoding plasmids. *C*, HEK293 cells were co-transfected with 0.5 μg of FLAG-IKKα and 0.5 μg of either pcDNA3Myc empty vector (*lane 1*) or the same amount of the indicated Myc-tagged PAN2 deletion mutants (*lanes 2–5*). Immunoprecipitations and kinase assays as well as immunoblot assays were performed as described above.

phosphorylation were suppressed in a concentration-dependent manner by PAN2. Similar results were obtained for IKKβ where PAN2 overexpression potentially suppressed IKKβ activity below base-line levels in TNFα-stimulated HEK293 cells (Fig. 7*B*).

To determine whether the PAAD domain of PAN2 is necessary for inhibition of IKKα activity, we compared the effects of full-length PAN2 with deletion mutants of PAN2 comprising the PAAD alone or lacking the PADD domain (ΔPAAD). As an additional control, a fragment of PAN2 representing only the LRRs was also tested. Plasmids encoding full-length and deletion mutants of PAN2 were transfected into 293 cells together with FLAG-tagged IKKα (in a 1:1 ratio), and kinase assays were performed as described above. As shown in Fig. 7*C*, both PAAD-only and ΔPAAD mutants inhibited IKKα activity (measured by *in vitro* phosphorylation of IKKα and GST-IκBα-(1–54)), although somewhat less potently than full-length PAN2. In contrast, a mutant encompassing only the LRR was almost inactive at suppressing IKKα activity, although all mutants were expressed to a comparable levels (Fig. 7*C*, *bottom panel*). We conclude that the PAAD domain is sufficient to suppress NF-κB, but other regions of the PAN2 protein can also interfere with cytokine-mediated induction of NF-κB.

DISCUSSION

This report provides evidence that the PAAD-containing protein PAN2 regulates NF-κB activity by affecting the IκB ki-

nases. Gene transfer-mediated increases in the levels of PAN2 suppressed NF-κB transcriptional activity in response to TNFα and IL-1β, implying that PAN2 operates at a point of convergence of these cytokine signal transduction pathways. Consistent with this hypothesis, PAN2 also suppressed induction of NF-κB activity by several signal transduction mediators within the TNF and IL-1 receptor pathways, including TRAF2, TRAF6, RIP, IRAK2, and Nik. Furthermore, PAN2 associates with IKKα and suppresses cytokine-mediated activation of this kinase, which plays a critical role in controlling degradation of IκB, thus releasing NF-κB. Although PAN2 did not associate with IKKβ in co-immunoprecipitation assays, it nevertheless suppressed its activation. This observation is consistent with reports that have suggested that IKKα operates upstream of IKKβ in some cytokine signaling pathways (25). At this point, we do not know whether the association of PAN2 with IKKα is direct *versus* indirect, requiring additional proteins analogous to the structurally similar CARD family proteins Nod1 and Nod2, which interact with the IKK complex indirectly via the adapter protein Cardiak (RIP2, Rick) (26). Indirect association might explain why only IKKα was co-immunoprecipitated with PAN2 instead of the entire IKK complex of IKKα, IKKβ, and IKKγ. In this regard, it is also possible that interaction of PAN2 with IKKα dissociates the IKK complex, explaining why PAN2 suppresses activation of both IKKα and IKKβ.

The architecture of PAN2 is similar to multiple proteins in animals and plants that contain various N-terminal effector domains followed by a NACHT domain and LRRs (27). The N-terminal effector domains range from CARDs in mammalian Nod1 (CARD4), Nod2 (inflammatory bowel disease protein 1), and CLAN (Ipaf, CARD12) to leucine zippers and Toll/IL-1 receptor domains in plants. Many of these proteins are presumably involved in innate immunity where their LRRs bind ligands produced by bacterial pathogens. For Nod1 and Nod2, for instance, it has been suggested that their LRRs bind lipopolysaccharide, triggering activation of the Nod1 and Nod2 proteins and inducing NF-κB (28, 29). One model for how these proteins become activated envisions the unliganded LRRs functioning as negative regulatory domains that suppress oligomerization of the NACHT domains until appropriate stimulatory ligands bind, relieving this autorepression. If PAN family proteins such as Cryopyrin and PAN2 operate in the same way, then we might expect their LRRs to recognize pathogen products, changing the activity state of these proteins. For this reason, we cannot exclude the possibility that PAN2 functions as a stimulator rather than inhibitor of NF-κB under some circumstances. However, as shown here, a truncation mutant of PAN2 lacking the LRRs suppressed (rather than enhancing) TNFα-mediated induction of NF-κB activity. Nevertheless, a recent report suggested that Cryopyrin can activate NF-κB when co-expressed with the PAAD/CARD protein ASC (30). In contrast, we have been unable to detect interactions of PAN2 with ASC.[3]

If PANs operate as suppressers of NF-κB *in vivo*, then one might speculate that the hereditary mutations associated with the PAN family protein Cryopyrin and the PAAD-containing protein Pyrin alter the functions of these proteins so that they are no longer capable of properly suppressing NF-κB, thereby explaining the hyperinflammatory syndromes associated with mutations in the genes encoding these proteins (21). We therefore speculate that at least some members of the PAAD family function in a negative feedback mechanism that ensures that NF-κB activity is produced in short bursts that limit inflammatory responses. It seems likely that PAADs may function as either inducers or suppressers of NF-κB depending on the balance of homotypic interactions between the PAAD domains of this large family of proteins, which presumably set thresholds within cells for NF-κB induction and inflammatory responses. In this regard, we analyzed the levels of endogenous PAN2 in HeLa and 293 cells after stimulation with TNFα, IL-1β, lipopolysaccharide, or phorbol 12-myristate 13-acetate, but no change in expression levels was observed (data not shown), suggesting that PAN2 protein is not induced by stimuli known to trigger NF-κB activation in these cell lines. Thus PAN2 activation may occur through a mechanism that involves modification of the protein at a post-translational level, its translocation in a particular cellular compartment, or its interactions with other proteins. Further work is needed to explore how PAN2 is regulated in response to inflammatory stimuli and to determine the specific biological contexts in which PAN2 operates.

[3] L. Fiorentino, C. Stehlik, and J. C. Reed, unpublished data.

Acknowledgments—We thank M. Karin (University of California San Diego) for valuable reagents and H. Chan, Y. Kim, J. Zapata, R. Newman, and G. Canettieri for helpful suggestions and discussions.

REFERENCES

1. Pawlowski, K., Pio, F., Chu, Z.-L., Reed, J. C., and Godzik, A. (2001) *Trends Biochem. Sci.* **26,** 85–87
2. Staub, E., Dahl, E., and Rosenthal, A. (2001) *Trends Biochem. Sci.* **26,** 83–85
3. Bertin, J., and DiStefano, P. S. (2000) *Cell Death Differ.* **7,** 1273–1274
4. Martinon, F., Hofmann, K., and Tschopp, J. (2001) *Curr. Biol.* **11,** R118–R120
5. Aravind, L., Dixit, V. M., and Koonin, E. V. (1999) *Trends Biochem. Sci.* **24,** 47–53
6. Ponting, C., Schultz, J., and Bork, P. (1997) *Trends Biochem. Sci.* **22,** 193–194
7. Consortium, T. I. F. (1997) *Cell* **90,** 797–807
8. Hoffman, H. M., Mueller, J. L., Broide, D. H., Wanderer, A. A., and Kolodner, R. D. (2001) *Nat. Genet.* **29,** 301–305
9. Masumoto, J., Taniguchi, S., Ayukawa, K., Sarvotham, H., Kishino, T., Niikawa, N., Hidaka, E., Katsuyama, T., Higuchi, T., and Sagara, J. (1999) *J. Biol. Chem.* **274,** 33835–33838
10. Chu, Z.-L., Pio, F., Xie, Z., Welsh, K., Krajewska, M., Krajewski, S., Godzik, A., and Reed, J. C. (2001) *J. Biol. Chem.* **276,** 9239–9245
11. Hlaing, T., Guo, R.-F., Dilley, K. A., Loussia, J. M., Morrish, T. A., Shi, M. M., Vincenz, C., and Ward, P. A. (2001) *J. Biol. Chem.* **276,** 9230–9238
12. Inohara, N., and Nunez, G. (2000) *Cell Death Differ.* **7,** 509–510
13. Koonin, E. V., and Aravind, L. (2000) *Trends Biol. Sci.* **25,** 223–224
14. Inohara, N., Koseki, T., Chen, S., Benedict, M. A., and Nunez, G. (1999) *J. Biol. Chem.* **274,** 270–274
15. Ogura, Y., Inohara, N., Benito, A., Chen, F. F., Yamaoka, S., and Nunez, G. (2001) *J. Biol. Chem.* **276,** 4812–4818
16. Damiano, J. S., Stehlik, C., Pio, F., Godzik, A., and Reed, J. C. (2001) *Genomics* **75,** 77–83
17. Li, W. Z., Pio, F., Pawlowski, K., and Godzik, A. (2000) *Bioinformatics* **16,** 1105–1110
18. Burge, C., and Karlin, S. (1997) *J. Mol. Biol.* **268,** 78–94
19. Matsuzawa, S., and Reed, J. C. (2001) *Mol. Cell* **7,** 915–926
20. Kim, Y., and Fischer, S. M. (1998) *J. Biol. Chem.* **273,** 27686–27694
21. Kastner, D. L., and O'Shea, J. J. (2001) *Nat. Genet.* **29,** 241–242
22. Ghosh, S., May, M. J., and Kopp, E. B. (1998) *Annu. Rev. Immunol.* **16,** 225–260
23. Silverman, N., and Maniatis, T. (2001) *Genes Dev.* **15,** 2321–2342
24. Karin, M., and Ben-Neriah, Y. (2000) *Annu. Rev. Immunol.* **18,** 621–663
25. OMahony, A., Lin, X., Geleziunas, R., and Greene, W. C. (2000) *Mol. Cell. Biol.* **20,** 1170–1178
26. Inohara, N., Ogura, Y., Chen, F. F., Muto, A., and Nuñez, G. (2000) *J. Biol. Chem.* **275,** 27823–27831
27. Dangl, J. L., and Jones, J. D. (2001) *Nature* **411,** 826–833
28. Inohara, N., Ogura, Y., Chen, F. F., Muto, A., and Nunez, G. (2001) *J. Biol. Chem.* **276,** 2551–2554
29. Hugot, J.-P., Chamaillard, M., Zouali, H., Lesage, S., Cezard, J.-P., Belaiche, J., Almer, S., Tysk, C., O'Morain, C. A., Gassull, M., Binder, V., Finkel, Y., Cortot, A., Modigllani, R., Laurent-Plug, P., Gower-Rousseau, C., Macry, J., Colombel, J.-F., Sahbatou, M., and Thomas, G. (2001) *Nature* **411,** 599–603
30. Manji, G. A., Wang, L., Geddes, B. J., Brown, M., Merriam, S., Al-Garawi, A., Mak, S., Lora, J. M., Briskin, M., Jurman, M., Cao, J., DiStefano, P. S., and Bertin, J. (2002) *J. Biol. Chem.* **277,** 11570–11575